Soft Matter

Triggered Interactions between Nanoparticles and Lipid Membranes: Design Principles for Gel Formation or Disruption-and-Release

Journal:	*Soft Matter*
Manuscript ID	SM-COM-06-2021-000864.R1
Article Type:	Communication
Date Submitted by the Author:	08-Jul-2021
Complete List of Authors:	Cao, Rui; University of Massachusetts, Department of Physics Gao, Jingjing; University of Massachusetts, Department of Chemistry Thayumanavan, Sankaran; University of Massachusetts, Department of Chemistry Dinsmore, Anthony; University of Massachusetts, Physics

Triggered Interactions between Nanoparticles and Lipid Membranes: Design Principles for Gel Formation or Disruption-and-Release

Rui Cao[†]*, Jingjing Gao*[†]*, S. Thayumanavan*[*]*, and Anthony D. Dinsmore* [*]
([†]Dr. R. Cao, Dr. J. Gao contributed equally to this work)
Dr. R. Cao, Prof. A.D. Dinsmore, *Department of Physics*
Dr. J. Gao, Prof. S. Thayumanavan, *Department of Chemistry*
University of Massachusetts Amherst, 01003, USA

E-mail: dinsmore@umass.edu, thai@chem.umass.edu

Keywords: triggered release, liposome, membrane disruption, nanoparticle, charge conversion

ABSTRACT: Lipid bilayer vesicles offer exciting possibilities for stimulated response, taking advantage of the membrane's flexibility and impermeability. We show how synergistic interactions between vesicles and polymer-based nanoparticles can be triggered at the nanoscale using UV light. This interaction leads either to adhesion and a membrane-based gel, or to nanoscale wrapping of the particles by the membrane and then vesicle destruction. To map the response, we varied the particle-membrane interactions *via* their surface charge densities. We found a crossover from adhesion to destruction at a well-defined region in parameter space. We modeled these results by accounting for the electrostatic attraction and the energy of membrane bending. We then synthesized amphiphilic polymers containing a UV-responsive nitrobenzyl moiety that switches its charge, and showed how a trigger predictably led to either a vesicle gel or disruption and release. The results pave the way to a new triggering mechanism and new response modes in soft materials.

INTRODUCTION

The lipid-bilayer membrane offers an enormous range of applications because it is thin, flexible, impermeable to most solutes, and fluid-like in its plane. Vesicles composed of lipid bilayers offer a wide range of potential for encapsulation of cargos (drugs, dyes, nutraceuticals) in their aqueous interiors. Incorporating responsive molecules or moieties into the membrane allows cargo release by enhancing membrane permeability through light,[1-7] temperature,[8-10] pH,[11] redox,[12] or enzyme.[13-14] Incorporation of responsive chemical functionalities in the lipid structure has been the most commonly used strategy to achieve these responsive characteristic. Recently, a very different approach for altering membrane permeability was reported, where membrane-binding nanoparticles induced either destruction of the vesicles and cargo release or vesicle-vesicle adhesion and formation of a solid gel.[15] There is a well-defined transition between these behaviors that depends on the strength of the particle-membrane interaction relative to the energy cost of bending the lipid membrane.[15-17] We are interested in whether this nanoparticle-membrane interaction can be turned on in response to a specific stimulus. We aim thereby to develop triggerable transitions from sol to vesicle-gel or *vice versa*, or rapid release of cargo encapsulated within the vesicles.

Toward this goal, we report here an amphiphilic block copolymer-based nanoparticle system that triggers rapid vesicle-vesicle adhesion or vesicle destruction, on demand, by means of an ultraviolet light (UV) stimulus (Fig. 1). The mechanism involves triggering the electrostatic interaction between lipid vesicles and nanoparticles, which triggers a change in morphology at the nanoscale that develops into a macroscopic response. To map the response of the nanoparticle-vesicle interaction, we used with nanoparticles self-assembled from amphiphilic polymers.[18] Each polymer consists of a hydrophobic block with a hexanyl coumarinyl methacrylate monomer and a hydrophilic block containing PEG_{112} with a terminus group that is charge-neutral (in **P0**) or cationic (**P1**). We varied the charge density of both the nanoparticles (by varying the relative fractions of **P0** and **P1**) and of the membranes (by mixing zwitterionic and anionic lipids). We found four distinct modes of response, ranging from vesicle-vesicle adhesion at relatively low charge densities to rapid vesicle rupture at high charge densities.

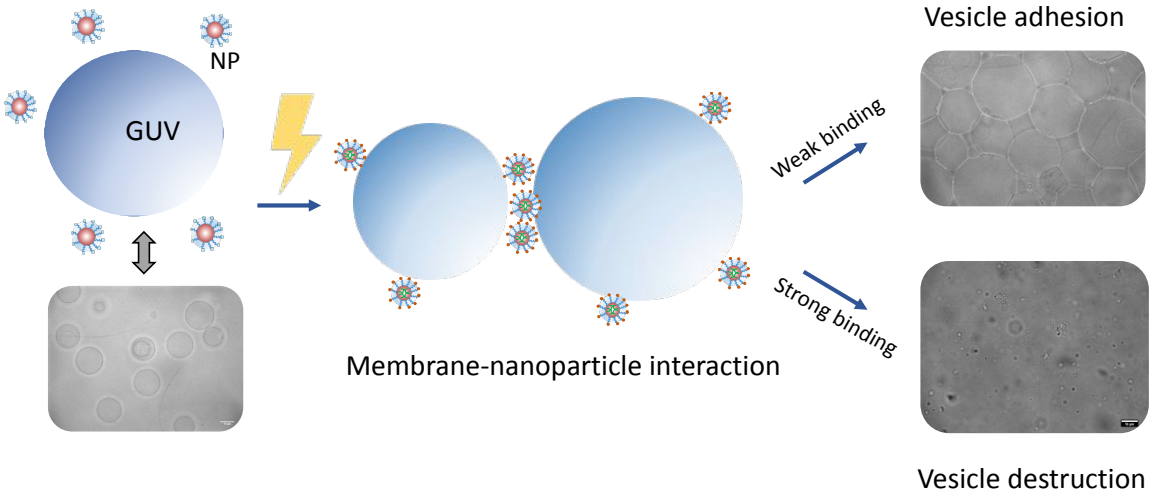

Figure. 1: Schematic illustration of the light-triggered particle adhesion and response.

Turning to a triggerable system, we synthesized a UV-sensitive polymer (**P2**) with a nitrobenzyl cap that switches the charge from neutral to positive on exposure to UV (equivalent to converting **P0** to **P1** with light). Correspondingly, in the presence of **P2**-based nanoparticles the vesicles either rapidly aggregated into a vesicle-gel structure or rapidly self-destructed upon exposure to light. The nature of the response depended on the charge density of the interacting assemblies. We successfully model our results by accounting for the attractive electrostatic double-layer interaction and the energy cost of deforming the membrane at the nanoscale. In addition to demonstrating the capability of light-triggered gelation or destruction-and-release, these results show how a multi-faceted or logic-gated response could be incorporated into this system.

RESULTS AND DISCUSSION

We first present the results with polymers and nanoparticles having a constant charge density (**P0**, **P1**), then turn our discussion to the UV-triggerable system (**P2**).

Neutral and cationic amphiphilic polymers and nanoparticles: Amphiphilic polymers, **P0 (**Mn 8.8 KDa, Đ 1.02.**)** and **P1 (**Mn 8.2 KDa, Đ 1.05) with molecular structure shown in Fig. 2(a), formed micellar nanoparticles in aqueous media (**NP0**, **NP1**). The average diameter of **NP0** and **NP1** was 125 nm, measured by dynamic light scattering (DLS, Fig. 2(b)). TEM images in Fig. 2(d) of drop-cast suspensions of **NP0** and **NP1** showed discrete particles with a size consistent with DLS. Figure 2(c) shows the zeta potential spectra of **NP0** and **NP1**, inferred from electrophoretic mobility measurements. The intensity-weighted mean values were -7.9 ± 6.9 mV for **NP0** and 13.0 ± 6.1 mV for **NP1**. (The uncertainty is the intensity-weighted standard deviation of the measurements.) The UV-triggerable polymer and nanoparticle (**P2**, **NP2**) will be described below.

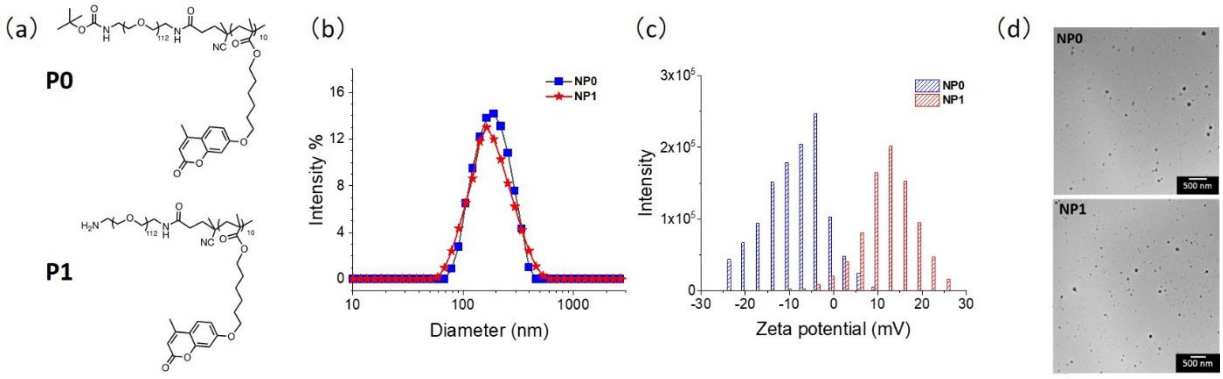

Figure. 2: (a) Molecular structures of amphiphilic diblock copolymers with hydrophilic blocks that are neutral (**P0**) or cationic (**P1**). (b) DLS size of micellar nanoparticles **NP0** and **NP1**. (c) Zeta potentials of **NP0** and **NP1**. (d) TEM images of drop-cast **NP0** and **NP1**.

States of particle-membrane interaction: To probe the interaction between membranes and nanoparticles, we explored the parameter space using self-assembled nanoparticles of varying charge densities. We made positive charged nanoparticles consisting of mixtures of **P0** and **P1** molecules. We refer to the mole fraction of **P1** as the fraction of amine termini, p_{amine} (relative to the total, including the nominally neutral **P0**). Giant unilamellar vesicles of roughly 10 μm radius

were composed of zwitterionic DOPC and anionic DOPG in different molar ratios. (See SI for details.) We refer to the molar fraction of DOPG as p_{DOPG}. Both p_{amine} and p_{DOPG} were set to 0, 25%, 50%, 75% and 100%. We exposed 20 μL of vesicle suspension to 5 μL of micellar nanoparticle suspension (0.5 mg/mL) in a perfusion chamber, and recorded the interaction under bright-field microscopy for at least 1 h. We explored 25 different combinations of p_{DOPG} and p_{amine}, with each combination repeated 2-3 times. In all cases, the vesicle interiors with 180 mOsm/L sucrose and the exteriors were a mixture of glucose and sucrose plus nanoparticles with a total osmolarity of 180 mOsm/L to avoid osmotic stress. Have sucrose inside the vesicles allowed them to gently sediment to the bottom and provided a refractive interest difference for viewing in the microscope.

We found four distinct particle-membrane interaction states as shown in Fig. 3(a-e). With p_{amine} = 0 (particles of **P0** only), we could discern no particle-membrane interactions; the vesicles were freely suspended and moved independently (Fig. 3(a)). With increasing p_{amine} and modest p_{DOPG}, we found adhesion of vesicles to one another (Fig. 3(b)), leading to a macroscopic gel phase. From dark-field optical microscopy, we found that particles bound to the membranes, where they acted as an adhesive bridge between vesicles (Fig. S1). The gel phase was stable over time, with no discernible rupture of the vesicles over a period of 2 h. Its structure was indistinguishable from vesicle-based gels obtained earlier with Au or silica nanoparticles[15] or oppositely charged polymers.[19] Recent shear rheology studies of those systems showed that the vesicle gel is a solid at low frequency.[15, 19]

With higher particle and membrane charge densities (Fig. 3(c)), we observed at least some of the vesicles burst into a compact residue with no visible interior lumen. The residue resembled a network of sub-μm tubules, which were flexible enough that thermal undulations were visible in the microscope. At the highest charge densities (Fig. 3(d)), we found that vesicles burst and then formed a more compact residue with no discernible thermal undulations. Figure 3(e) shows a common case that coexisted with that of Fig. 3(d): given two adhered vesicles, one of them would burst and leave a ring of residue on the other vesicle, in the form of a spherical cap. The presence or absence of these behaviors was repeatable in samples with the same composition. We emphasize that the boundary between these responses was sharp and well defined. We return to this point below.

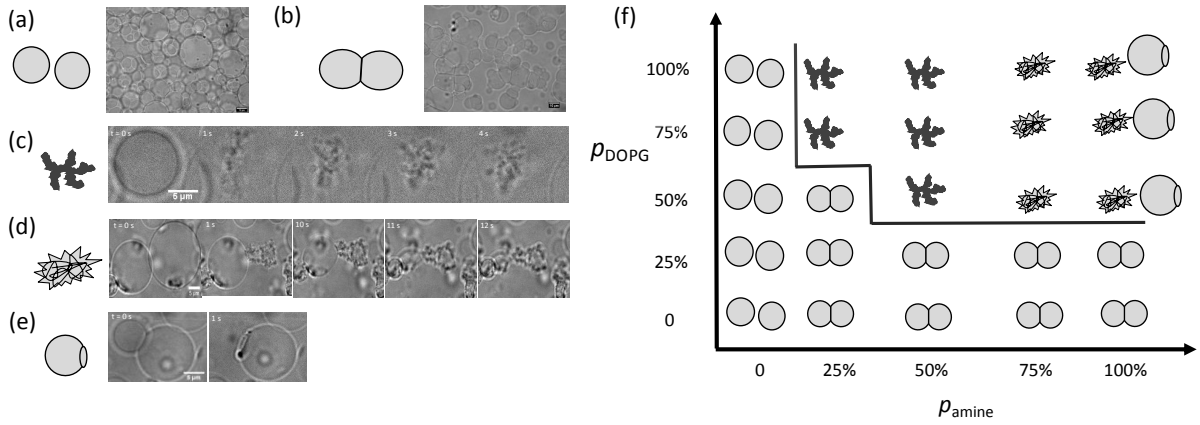

Figure. 3: Four distinct states of particle-membrane interaction. (**a**) Free vesicle state. (**b**) Vesicle-vesicle adhesion. (**c**) Vesicles burst into flexible residue. (**d**) Vesicles burst into compact aggregates. (**e**) One vesicle burst and leaves a

spherical cap on a neighboring vesicle. (**f**) State diagram shows the results one hour after mixing, with each icon showing results of repeated experiments.

These behaviors are summarized in a state diagram in Fig. 3(f). The states that are defined as rupture (Fig. 3(c,d,e)) are those in which at least some vesicles were seen to undergo rupture. The states varied systematically with the values of both p_{DOPG} and p_{amine}. For example, with p_{amine} fixed at 50% and varying p_{DOPG}, we found a trend from vesicle-vesicle adhesion to vesicle rupture as a flexible residue when p_{DOPG} reached 50%. On the other hand, when we kept p_{DOPG} at 50%, we observed no interaction at $p_{amine} = 0$, vesicle-vesicle adhesion at $p_{\mathrm{amine}} = 25\%$, vesicle rupture and flexible residue at $p_{\mathrm{amine}} = 50\%$, and vesicle rupture with compact residue at $p_{\mathrm{amine}} = 75\%$ and 100%. We also observed that roughly 1 out of 20 surviving vesicles showed the spherical cap (as in Fig. 3(e)) at $p_{\mathrm{amine}} = 100\%$.

The vesicle-vesicle adhesion began approximately 20-40 s after particles were added to vesicles. For the flexible-residue rupture case, we observed at least 1 out of 100 vesicles ruptured. For example, at $p_{\mathrm{amine}} = 25\%$, $p_{\mathrm{DOPG}} = 75\%$, roughly 1 out of 50 vesicles were observed to rupture as flexible residue. We typically observed no apparent change for up to 30 s, followed by a rapid rupture process within 1 s. In cases with $p_{\mathrm{amine}} = 100\%$, $p_{\mathrm{DOPG}} = 100\%$, 1 out 20 vesicles ruptured as compact residue within 1 s, starting about 40 s after particle addition. Below, we describe experiments with a higher particle concentration that show a higher fraction of vesicles destroyed, indicating that the number of particles limits the total destruction. We return to this point near the end of the discussion.

UV-triggerable amphiphilic polymers and nanoparticles: To achieve triggerable nanoparticle-membrane interactions, we prepared nanoparticle **NP2** from a light-senstive polymer **P2** (Mn 8.2 K Da, Đ 1.05), which provides the opportunity to tune the surface charge through the UV-cleavable nitrobenzyl group[19-20] (Fig. 4(a)). Like **P0** and **P1**, **P2** formed nanoparticles in aqueous solution. When an **NP2** solution was exposed to UV light, we found that the zeta potential of the nanoparticle converted from -4.1 ± 5.8 mV to 7.7 ± 4.5 mV (Fig. 4(b)), indicating the UV light successfully cleaved the nitrobenzyl group to generate a primary amine. This was also confirmed by the absorbance increase at 400 nm corresponding to the formation of nitrosobenzaldehyde byproduct from the photoinduced degradation of the nitrobenzylcarbamate (Fig. S2). Also note that the hydrophobic core of **NP2** was concurrently crosslinked in the presence of UV light to generate a stable nanoparticle because of the coumarin dimerization, as discerned by the absorbance decrease at 320 nm (Fig. S2).[20-21] The DLS spectrum (Fig. S3) and TEM images (Fig. S4) indicate that the morphology of **NP2** did not change in a detectable way after UV exposure and that all of the nanoparticles had a similar size distribution. With UV exposure, **NP2** switched its zeta potential from slightly negative (**NP0**-like) to positive (**NP1**-like) (Fig. 4(b)). **NP2** therefore allowed us to switch our system from one state to another in the diagram of Fig. 3(f).

Triggered particle-membrane interactions: To trigger vesicle-vesicle adhesion, we mixed 100 μL of vesicle suspension ($p_{\mathrm{DOPG}} = 0$) and 200 μL of **NP2** (0.5 mg/mL) suspension having the same osmolarity. We then split the mixture into control (150 μL) and experiment (150 μL) groups. We observed that vesicles in the control group (no UV) remained freely suspended with no intensity enhancement detected in dark-field microscopy and no vesicle adhesion detected even after 24 h. On the contrary, after being sealed in a chamber to prevent water evaporation, the experiment group was exposed to UV (wavelength 365 nm, power 15 W for 10 min), after which we observed vesicle-vesicle adhesion throughout the sample as shown in Fig. 4(c). In terms of Fig. 3(f), this

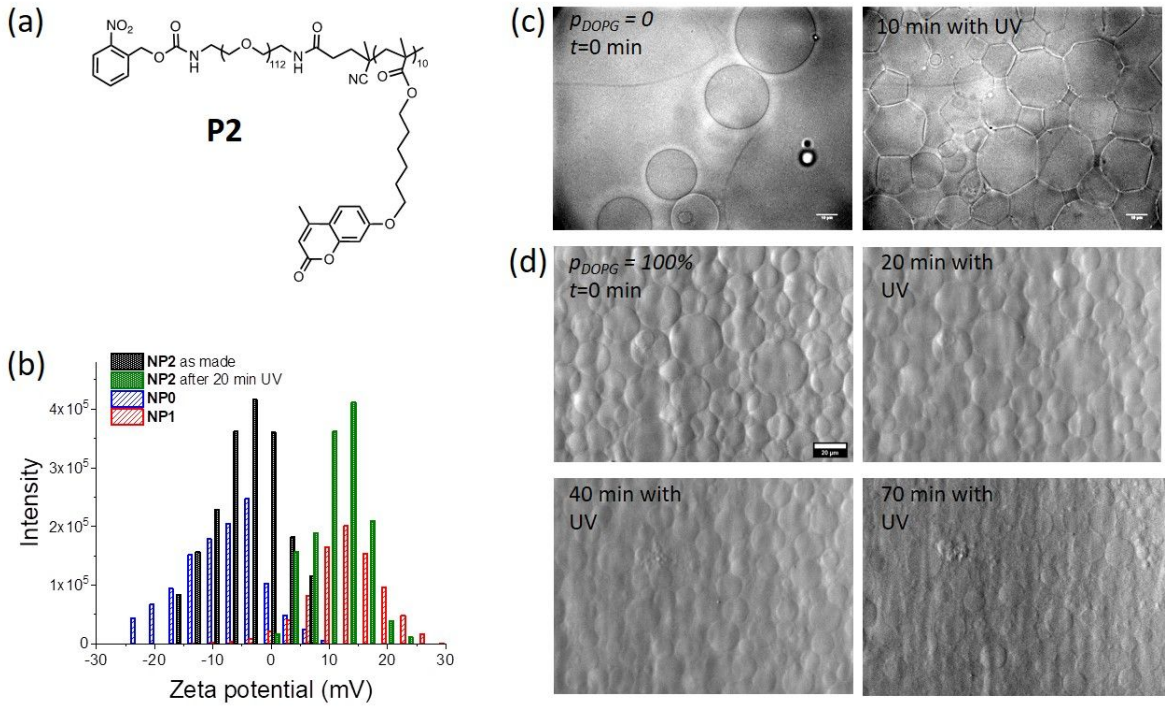

Figure. 4: (a) Molecular structures of the UV-triggerable amphiphilic diblock copolymer, **P2**. (b) Zeta potentials of **NP2** show the switch induced by UV exposure. Corresponding data for **NP0** and **NP1** are shown for comparison. (c) Bright-field optical images of triggered adhesion of vesicles with p_{DOPG} =0 mixed with **NP2**. UV was turned on at t = 0. (d) Time sequence of UV-triggered vesicle destruction of vesicles with p_{DOPG} =100%, mixed with **NP2**. UV was turned on at t=0.

experiment corresponds to rapidly shifting from p_{amine}, p_{DOPG} = (0,0) to (100%, 0). The observed final state is indistinguishable from what we reported in the steady-state experiments of Fig. 3.

To trigger vesicle rupture, we set p_{DOPG} = 100%. After carefully depositing 1 μL vesicle suspension in the chamber filled with 300 μL **NP2** suspension (in glucose solution with the same osmolarity), we exposed the sample to UV (wavelength 365 nm, power density 8 mW/cm^2) continuously while acquiring bright-field images (Fig. 4(d)). We observed clear vesicle rupture and a dramatic decrease in the number of intact vesicles over time. From image analysis, we found that 83 out of the initial 124 vesicles ruptured within 70 min. Among the remaining intact vesicles, we also noted a reduction of image contrast between the inside and outside of the vesicles. This observation confirms release of sucrose solution from inside the ruptured vesicles, leading to a closer match of the interior and exterior refractive indices.

Mechanism of binding, deformation, and destruction: The binding response arose from electrostatic attraction between the membrane and the nanoparticles. Previous work showed that the zeta potential of DOPC/DOPG vesicles is tunable using p_{DOPG} (at 0, 20%, and 100%, zeta potentials were approximately -8, -70 and -80 mV, respectively, with ~10 mM NaCl[22]). With nanoparticles composed of **P0** (p_{amine} = 0), the charge was near zero and the interaction between lipid membranes and nanoparticles was weak. Irrespective of p_{DOPG}, vesicles moved freely with **NP0**. After increasing p_{amine} to ≥ 25%, the nanoparticles were sufficiently positively charged, leading to a double-layer interaction with the negatively charged membrane.

When the attractive interaction strength was moderate (*e.g.*, p_{amine} = 25% and p_{DOPG} = 25%), nanoparticles bound to the membranes. Dark-field optical images (Fig. S1) showed that the intensity of light scattered by particles bound on a membrane was approximately 12× greater than scattered from the membrane alone. Furthermore, the concentration of membrane-bound particles was greater by a factor of 1.7 ± 0.2 between two membranes compared to at one free membrane. (See SI for details.) This enhancement indicates that particles were attracted to the adhesion spots where they could bind to both membranes. Figure 5(a) illustrates the adhesion mechanism. This enhancement factor is close to the value of 2 that is expected from theory if the particle concentration were tuned to maximize the inter-vesicle adhesion.[23] No thermal motion of vesicles was observed, which indicates strong adhesion energy relative to the thermal energy.

When the attractive interaction was strong (*e.g.*, p_{amine} = 25% and p_{DOPG} = 100%), nanoparticles induced rupture of the vesicles. We attribute this rupture to strong binding and compete wrapping of the particles by the membrane at the nanoscale, as illustrated in Fig. 5(b). When a particle binds to the membrane, the membrane tends to wrap the particle, driven by the binding energy per area of contact, w. Deformation of the membrane is suppressed by the membrane's bending modulus κ, the tension τ,[16, 24-28] or osmotic pressure.[29] When the binding predominates, an individual particle is completely wrapped by the membrane.[15-16, 30-32] For a single spherical particle of radius a having short-ranged attraction and binding to membranes with low tension ($\tau a^2/\kappa \ll 1$), there is a predicted sharp transition from weak deformation to wrapping. The transition occurs when wa^2/κ exceeds a threshold of 2.[16] When many spherical particles are present, the deformed membrane induces in-plane particle interactions, which can amplify the membrane response and cause large-scale remodeling. [33-37] (Cooperative effects are also seen among non-spherical particles including proteins.[26-27, 32, 38-41]) Recent simulations showed that in the regime of many spherical particles, the threshold to wrapping is reduced to $wa^2/\kappa \approx 0.5$.[15]

As more particles bind and are wrapped, the membrane must stretch to encompass the vesicle interior volume, so that tension rises and eventually the vesicle bursts.[42] Bursting leaves a composite membrane-nanoparticle residue whose features are too small to resolve. Finally, the crossover from flexible residue to rigid residue (Fig. 3(f)) is attributed to a greater concentration of bound particles with greater p_{amine}. We speculate that in such conditions, the membrane surface may become jammed by particles and thereby develop a rigid surface.

We propose a straightforward continuum-level model to predict the conditions leading to the triggered rupture. We used the Debye-Hückel model for the electrostatic double-layer interaction to estimate the binding energy per area w. When the distance between the particle surface and the membrane (h) is much smaller than the Debye screening length l_{D}, it is reasonable to regard both membrane and particle as flat plates with surface potentials ψ_m and ψ_p (Fig. S5). The adhesion free energy per area, w, is estimated as $w = (2\varepsilon\varepsilon_0/l_{\text{D}})\,\psi_p\psi_m \exp(-h/l_{\text{D}})$.[43] We assumed that both ψ_p and ψ_m increased linearly with p_{amine} and p_{DOPG} and used our electrophoretic mobility measurements to estimate their values. We then found the set of points in the (p_{amine}, p_{DOPG}) plane where $wa^2/\kappa = 0.5$, the estimated onset of wrapping and destruction with many particles.[15] Owing to the uncertainty in the measured surface potentials, we obtained a range of results corresponding

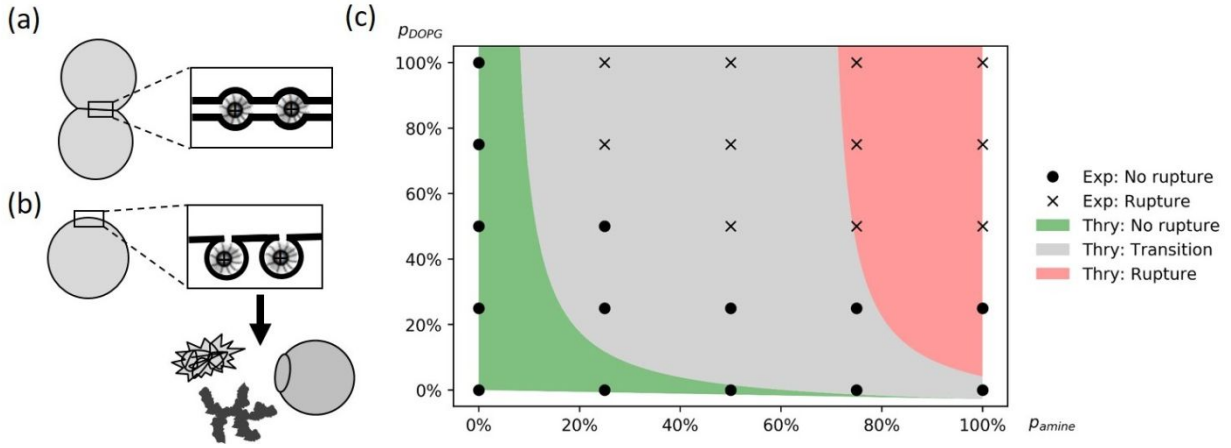

Figure. 5: The cross-over from weak binding, illustrated in (**a**), to strong binding where the membrane fully wraps leading to rupture (**b**). (**c**) Predicted cross-over from adhesion to wrapping. The cross-over is expected to be sharp and the width of the gray region accounts for uncertainties in the physical parameters. Symbols: ● are measured points of adhesion; × are measured points of wrapping and destruction.

to this predicted transition; details are given in the supplementary section. The calculation and the experimental results are plotted together in Fig. 5(c). We found that the model successfully captures the data trend despite the model's simplicity. The model shows how future systems could be designed with this approach.

In the model, we implicitly assumed that tension was negligible, *i.e.*, that $\tau a^2/\kappa \ll 1$. For our system ($a = 60$ nm, $\kappa \approx 10^{-19}$ J[44]), this condition requires $\tau \ll 30$ μN/m. Tension at that low scale can be realized in vesicles that are slightly deflated by osmotic stress.[33] Such vesicles have clearly visible thermal undulations of their shape, whereas vesicles with τ in the mN/m scale appear spherical in shape (like typical GUVs in our experiments). This leaves open the question of how τ affects binding and wrapping. Here we speculate that when particles bind to a tense membrane, they locally strain it and enhance permeability to water and solute.[45] By this mechanism, τ would decrease over time until the above condition is met and the particles are completely wrapped. This mechanism would explain the approximately 30 s time lag that we observed between particle addition and vesicle destruction.

In the triggered-response experiments of Fig. 4, we found that the majority of vesicles were destroyed. By contrast, in the exploration of the state diagram of Fig. 3, a smaller fraction was destroyed. We attribute this difference to the total quantity of particles in the sample relative to the amount of exposed membrane area. For Fig. 4(c,d), the estimated particle concentration was 4×10^{13}/mL, so that the total particle surface area was roughly 3×10^4 cm^2/mL. For the vesicles (10 μm radius), we assumed a close-packed volume fraction and estimated the membrane surface area as 2×10^3 cm^2/mL. There were therefore roughly 10× more particles than were needed to entirely cover all of the exposed membrane. For the data of Fig. 3, by contrast, the particles were present at approximately 1,000× lower concentration, which explains the smaller fraction of destroyed vesicles.

SUMMARY

In summary, we showed that the response of the vesicles could be rationally tuned between liquid suspension, solid gel, or destruction-and-release by means of the surface charge densities of the membrane and nanoparticles. Using this scheme, we then demonstrated UV-stimulated transitions

from liquid to vesicle-gel and from liquid to destruction-and-release. The destruction begins with a wrapping transition at the scale of individual particles and extends to macroscale as the membrane ruptures and releases its contents. These results allow us to design amphiphile-based systems that can be designed to respond in specific ways depending on the stimulus. By extension of our results, it should be possible to trigger either gel formation or total destruction by means of the light intensity or by varying the amount of responsive block copolymer in the nanoparticle, which determines the value of p_{amine}. If the vesicles had a narrow size distribution, then triggered particle-induced adhesion may lead to new symmetries in the packing of the vesicles, determined by the conditions of fixed vesicle interior volume but flexible shape. We also anticipate materials that could respond to different triggers in disparate ways. For example, vesicles with 10% DOPG could be mixed with two or more kinds of particles that have different p_{amine} (*e.g.*, 20% and 90%) and that respond to different triggers, so that gel formation or destruction-and-release follow from separate triggers. Alternatively, vesicles with two different compositions and containing two different cargoes could be mixed with particles that would cause gel formation by some of the vesicles, together with disruption of the other ones. Overall, the findings here create new opportunities for programmable molecular release applications.

Supporting Information:
Materials and methods; NMR spectra of **P0**, **P1** and **P2**; dark-field images of bound nanoparticles; absorption spectra; particle sizes by DLS and TEM images; details of the theoretical prediction for the adhesion-to-destruction crossover.

Acknowledgments:
We thank the Army Research Office for funding through the MURI program, grant W911NF-15-1-0568. We also thank Arash Manafirad with assistance in the UV exposure experiments and Sarah Zuraw-Weston for helpful discussions.

Cited references:

1. Kano, K.; Tanaka, Y.; Ogawa, T.; Shimomura, M.; Kunitake, T., Photoresponsive Artificial Membrane - Regulation of Membrane-Permeability of Liposomal Membrane by Photoreversible cis-trans Isomerization of Azobenzenes. *Photochem. Photobiol.* **1981,** *34* (3), 323-329.
2. Bisby, R. H.; Mead, C.; Morgan, C. G., Photosensitive liposomes as 'cages' for laser-triggered solute delivery: the effect of bilayer cholesterol on kinetics of solute release. *FEBS Lett.* **1999,** *463* (1-2), 165-168.
3. Lei, Y. B.; Hurst, J. K., Photoregulated potassium ion permeation through dihexadecyl phosphate bilayers containing azobenzene and stilbene surfactants. *Langmuir* **1999,** *15* (10), 3424-3429.
4. Kuiper, J. M.; Engberts, J. B. F. N., H-aggregation of azobenzene-substituted amphiphiles in vesicular membranes. *Langmuir* **2004,** *20* (4), 1152-1160.
5. Diguet, A.; Yanagisawa, M.; Liu, Y. J.; Brun, E.; Abadie, S.; Rudiuk, S.; Baigl, D., UV-Induced Bursting of Cell-Sized Multicomponent Lipid Vesicles in a Photosensitive Surfactant Solution. *J. Am. Chem. Soc.* **2012,** *134* (10), 4898-4904.
6. Molla, M. R.; Rangadurai, P.; Antony, L.; Swaminathan, S.; de Pablo, J. J.; Thayumanavan, S., Dynamic actuation of glassy polymersomes through isomerization of a single azobenzene unit at the block copolymer interface. *Nat. Chem.* **2018,** *10* (6), 659-666.
7. Liu, Y. Y.; An, X. Q., Preparation, microstructure and function of liposome with light responsive switch. *Colloid Surf. B-Biointerfaces* **2019,** *178*, 238-244.
8. Li, L.; ten Hagen, T. L. M.; Schipper, D.; Wijnberg, T. M.; van Rhoon, G. C.; Eggermont, A. M. M.; Lindner, L. H.; Koning, G. A., Triggered content release from optimized stealth thermosensitive liposomes using mild hyperthermia. *J. Control. Release* **2010,** *143* (2), 274-279.
9. Papahadjopoulos, D.; Jacobson, K.; Nir, S.; Isac, T., Phase Transitions in Phopholiopid Vesicles - Fluorescence Polarization and Permeability Measurements Concerning Effect of Temperature and Cholesterol. *Biochimica Et Biophysica Acta* **1973,** *311* (3), 330-348.
10. Ta, T.; Porter, T. M., Thermosensitive liposomes for localized delivery and triggered release of chemotherapy. *J. Control. Release* **2013,** *169* (1-2), 112-125.
11. Paliwal, S. R.; Paliwal, R.; Vyas, S. P., A review of mechanistic insight and application of pH-sensitive liposomes in drug delivery. *Drug Deliv.* **2015,** *22* (3), 231-242.
12. Loew, M.; Forsythe, J. C.; McCarley, R. L., Lipid Nature and Their Influence on Opening of Redox-Active Liposomes. *Langmuir* **2013,** *29* (22), 6615-6623.
13. Zhu, L.; Kate, P.; Torchilin, V. P., Matrix Metalloprotease 2-Responsive Multifunctional Liposomal Nanocarrier for Enhanced Tumor Targeting. *ACS Nano* **2012,** *6* (4), 3491-3498.
14. Elegbede, A. I.; Banerjee, J.; Hanson, A. J.; Tobwala, S.; Ganguli, B.; Wang, R. Y.; Lu, X. N.; Srivastava, D. K.; Mallik, S., Mechanistic studies of the triggered release of liposomal contents by matrix metalloproteinase-9. *J. Am. Chem. Soc.* **2008,** *130* (32), 10633-10642.
15. Zuraw-Weston, S.; Wood, D. A.; Torres, I. K.; Lee, Y.; Wang, L. S.; Jiang, Z.; Lázaro, G. R.; Wang, S.; Rodal, A. A.; Hagan, M. F.; Rotello, V. M.; Dinsmore, A. D., Nanoparticles binding to lipid membranes: from vesicle-based gels to vesicle tubulation and destruction. *Nanoscale* **2019,** *10*, 18464-18474.
16. Deserno, M., Elastic deformation of a fluid membrane upon colloid binding. *Phys. Rev. E* **2004,** *69* (3), 031903.
17. Dietrich, C.; Angelova, M.; Pouligny, B., Adhesion of latex spheres to giant phospholipid vesicles: Statics and dynamics. *J. Phys. II* **1997,** *7* (11), 1651-1682.
18. Gao, J. J.; Wu, P. D.; Fernandez, A.; Zhuang, J. M.; Thayumanavan, S., Cellular AND Gates: Synergistic Recognition to Boost Selective Uptake of Polymeric Nanoassemblies. *Angew. Chem.-Int. Edit.* **2020,** *59* (26), 10456-10460.
19. Cao, R.; Kumar, D.; Dinsmore, A. D., A Vesicle-based Gel via Polyelectrolyte-Induced Adhesion: Structure, Rheology, and Response. *Langmuir* **2021,** *37*, 1714-1724.

20. Holmes, C. P.; Jones, D. G., Reagents for Combinatorial Organic Synthesis - Development of a New O-Nitrobenzyl Photolabile Linker for Solid-Phase Synthesis. *J. Org. Chem.* **1995,** *60* (8), 2318-2319.
21. Gao, J. J.; Liu, X. C.; Secinti, H.; Jiang, Z. W.; Munkhbat, O.; Xu, Y. S.; Guo, X. H.; Thayumanavan, S., Photoactivation of Ligands for Extrinsically and Intrinsically Triggered Disassembly of Amphiphilic Nanoassemblies. *Chem.-Eur. J.* **2018,** *24* (8), 1789-1794.
22. Maity, P.; Saha, B.; Kumar, G. S.; Karmakar, S., Binding of monovalent alkali metal ions with negatively charged phospholipid membranes. *Biochim. Biophys. Acta-Biomembr.* **2016,** *1858* (4), 706-714.
23. Stieger, T.; Schoen, M.; Weikl, T. R., Adhesion of surfaces mediated by adsorbed particles: Monte Carlo simulations and a general relationship between adsorption isotherms and effective adhesion energies. *Soft Matter* **2012,** *8* (46), 11737-11745.
24. Le Bihan, O.; Bonnafous, P.; Marak, L.; Bickel, T.; Trepout, S.; Mornet, S.; De Haas, F.; Talbot, H.; Taveau, J. C.; Lambert, O., Cryo-electron tomography of nanoparticle transmigration into liposome. *J. Struct. Biol.* **2009,** *168* (3), 419.
25. Bahrami, A. H.; Raatz, M.; Agudo-Canalejo, J.; Michel, R.; Curtis, E. M.; Hall, C. K.; Gradzielski, M.; Lipowsky, R.; Weikl, T. R., Wrapping of nanoparticles by membranes. *Adv. Colloid Interface Sci.* **2014,** *208*, 214-224.
26. Franquelim, H. G.; Khmelinskaia, A.; Sobczak, J. P.; Dietz, H.; Schwille, P., Membrane sculpting by curved DNA origami scaffolds. *Nat. Commun.* **2018,** *9*, 811.
27. Reynwar, B. J.; Illya, G.; Harmandaris, V. A.; Muller, M. M.; Kremer, K.; Deserno, M., Aggregation and vesiculation of membrane proteins by curvature-mediated interactions. *Nature* **2007,** *447* (7143), 461.
28. Adriani, G.; de Tullio, M. D.; Ferrari, M.; Hussain, F.; Pascazio, G.; Liu, X. W.; Decuzzi, P., The preferential targeting of the diseased microvasculature by disk-like particles. *Biomaterials* **2012,** *33* (22), 5504-5513.
29. Yu, Q. F.; Dasgupta, S.; Auth, T.; Gompper, G., Osmotic Concentration-Controlled Particle Uptake and Wrapping-Induced Lysis of Cells and Vesicles. *Nano Lett.* **2020,** *20* (3), 1662-1668.
30. Dasgupta, S.; Auth, T.; Gompper, G., Shape and Orientation Matter for the Cellular Uptake of Nonspherical Particles. *Nano Lett.* **2014,** *14* (2), 687-693.
31. Spangler, E. J.; Laradji, M., Discontinuous wrapping transition of spherical nanoparticles by tensionless lipid membranes. *J. Chem. Phys.* **2020,** *152* (10), 104902.
32. Johannes, L.; Parton, R. G.; Bassereau, P.; Mayor, S., Building endocytic pits without clathrin. *Nat. Rev. Mol. Cell Biol.* **2015,** *16* (5), 311-321.
33. van der Wel, C.; Vahid, A.; Saric, A.; Idema, T.; Heinrich, D.; Kraft, D. J., Lipid membrane-mediated attraction between curvature inducing objects. *Sci. Rep.* **2016,** *6*, 32825.
34. Saric, A.; Cacciuto, A., Mechanism of Membrane Tube Formation Induced by Adhesive Nanocomponents. *Phys. Rev. Lett.* **2012,** *109* (18), 188101.
35. Bahrami, A. H.; Lipowsky, R.; Weikl, T. R., Tubulation and Aggregation of Spherical Nanoparticles Adsorbed on Vesicles. *Phys. Rev. Lett.* **2012,** *109* (18), 188102.
36. Raatz, M.; Lipowsky, R.; Weikl, T. R., Cooperative wrapping of nanoparticles by membrane tubes. *Soft Matter* **2014,** *10* (20), 3570-3577.
37. Xiong, K.; Zhao, J. Y.; Yang, D. W.; Cheng, Q. W.; Wang, J. L.; Ji, H. B., Cooperative wrapping of nanoparticles of various sizes and shapes by lipid membranes. *Soft Matter* **2017,** *13* (26), 4644-4652.
38. McMahon, H. T.; Gallop, J. L., Membrane curvature and mechanisms of dynamic cell membrane remodelling. *Nature* **2005,** *438* (7068), 590-596.
39. Mellor, H., The role of formins in filopodia formation. *Biochim. Biophys. Acta-Mol. Cell Res.* **2010,** *1803* (2), 191-200.
40. Reynwar, B. J.; Deserno, M., Membrane-mediated interactions between circular particles in the strongly curved regime. *Soft Matter* **2011,** *7* (18), 8567.

41. Qualmann, B.; Koch, D.; Kessels, M. M., Let's go bananas: revisiting the endocytic BAR code. *EMBO J.* **2011,** *30* (17), 3501-3515.
42. Linklater, D. P.; Baulin, V. A.; Le Guevel, X.; Fleury, J. B.; Hanssen, E.; Nguyen, T. H. P.; Juodkazis, S.; Bryant, G.; Crawford, R. J.; Stoodley, P.; Ivanova, E. P., Antibacterial Action of Nanoparticles by Lethal Stretching of Bacterial Cell Membranes. *Adv. Mater.* **2020,** *32* (52), 2005679.
43. Russel, W. B.; Saville, D. A.; Schowalter, W., *Colloidal Dispersions*. Cambridge U. Press: 1989.
44. Nagle, J. F.; Jablin, M. S.; Tristram-Nagle, S.; Akabori, K., What are the true values of the bending modulus of simple lipid bilayers? *Chem. Phys. Lipids* **2015,** *185*, 3-10.
45. Li, S.; Malmstadt, N., Deformation and poration of lipid bilayer membranes by cationic nanoparticles. *Soft Matter* **2013,** *9* (20), 4969-4976.